Optimization of Food Transportation and Storage in an Insulated Box: Effect of Phase Change Material Position and Spacing Underneath the Load Tanathep Leungtongkum* (a, b) , Denis Flick (b) , Hong Minh Hoang (a) , Duret Steven (a) , Anthony Delahaye (a) and Onrawee Laguerre (a)

Tanathep Leungtongkum, D. Flick, Hong-Minh Hoang, Steven Duret,
Anthony Delahaye, Onrawee Laguerre

HAL Id: hal-04198851
https://hal.inrae.fr/hal-04198851

Submitted on 7 Sep 2023

Optimization of Food Transportation and Storage in an Insulated Box: Effect of Phase Change Material Position and Spacing Underneath the Load

Tanathep Leungtongkum*[a, b], Denis Flick[b], Hong Minh Hoang[a], Duret Steven[a], Anthony Delahaye[a] and Onrawee Laguerre[a]

[a]Université Paris-Saclay, INRAE, FRISE, 92761, Antony, France
[b]Université Paris-Saclay, INRAE, AgroParisTech, UMR SayFood, 91300 Massy, France
*Corresponding author e-mail: tanathep.leungtongkum@inrae.fr

ABSTRACT

Food transport and storage in an insulated box equipped with Phase Change Material (PCM) is common for last mile delivery; however, it was addressed as a weak link with high average temperature and high temperature heterogeneity. This experimental study investigated the effect of PCM position (at the lid and at a side wall) and the spacing underneath the load on the temperature profiles inside the box. PCM (water-based), air, surface and core temperatures of the load (test product made of methylcellulose) at different positions were measured every 30 seconds from loading until PCM totally melted. PCM position is a determining factor on the coldest and warmest position while the underneath space decreased the difference between the maximum and minimum core temperature. In spite that the average temperature was not affected by these factors, the presence of space below the load is essential for temperature homogeneity.

Keywords: Food, Transport, Storage, Phase Change Material, Optimization

1. INTRODUCTION

Insulated boxes equipped with Phase Change Material (PCM) allow to preserve temperature sensitive products during transportation and storage. Despite its simple implementation and low cost, maintaining of recommended temperature is a challenge since temperature abuse was often observed in practice (Laguerre et al., 2013; Mercier et al., 2017). Thus, optimization of box configuration is necessary to reduce food waste.

PCM position is a factor affecting temperature profile inside the box. Du et al. (2020) investigated the effect of PCM position in an empty box and recommended to put PCM on top and at 4 side walls. If the PCM position is inappropriate, the temperature difference between the minimum and the maximum values may be higher than that without PCM although the average temperature is lower in the case with PCM (Navaranjan et al., 2013).

The presence of air space (allowed by a perforated support) beneath the load is recommended to reduce the temperature heterogeneity thanks to better convective heat transfer (Hundy et al., 2008). This practice is often used for the transport and storage in cold equipment with active cooling unit. For food transport in an insulated box, the users tend to fill the load as much as possible with small air space inside to achieve profitability under the small volume constraint (East & Smale, 2008). For the sake of food quality, determination of the effect of spacing beneath the load would be useful to develop stakeholder guideline for food transportation in an insulated box with PCM. According to authors' knowledge, there is no study on the effect of air space beneath the load in a system without active cooling unit where only free convection occurs.

The objective of this work is to find out the effect of PCM position and the spacing beneath the load on temperature profile of an insulated box loaded with products. The optimal configuration concerning these two factors is proposed. The results of this thermal study are complementary to the ones of airflow pattern inside the box (results not shown here). A better knowledge of coupled heat transfer and airflow in an

insulated boxes can allow to propose technical solutions to maintain an appropriated product temperature along the logistic chain.

2. MAIN SECTION

2.1. Materials and methods

2.1.1. Insulated box, PCM and load

The studied box was multilayer insulated (Manutan SA, Gonesse, France) with 510 mm x 310 mm x 300 mm internal dimension and 580 mm x 380 mm x 380 mm external dimension (Fig 1a). The side and bottom walls are composed of expanded polystyrene (25 mm thickness), polypropylene (inner and outer layers of 3.5 mm thickness) and air gap between expanded polystyrene and inner layer (5 mm thickness). The box was placed over a wood supports of 50 mm height to assure an even heat exchange between the ambient air and all box's walls (Fig. 1b). This box is on a table (0.7 m height) located at the centre of the test room of 3.4 m x 3.4 m x 2.5 m in which the ambient temperature was controlled at 20°C. Four kg of tap water (melting point ~ 0°C) was filled in PCM slab with 480 mm x 281 mm x 35 mm external dimension (walls in polypropylene of 2.5 mm thickness). The test product (16 packs, dimension of a pack 200 mm x 100 mm x 50 mm) were arranged in the box (Fig 1c - front view, Fig 1d - side view and Fig 1e – top view), the composition of the test product is 23% methylhydroxyethylcellulose, 76.4% water and 0.5% NaCl (Refrigeration Development and Testing Ltd., North Somerset, UK). With this configuration and due to a simple heat balance, the box would be able to keep the test product temperature below 8°C for about 28 hours. The load was placed on a perforated support to create spacing beneath. This support was made of galvanized steel with the cross section of 350 mm x 150 mm and the height of 20 mm.
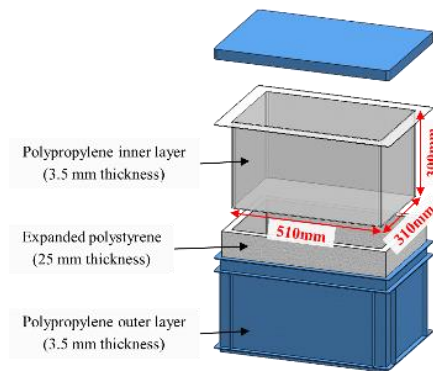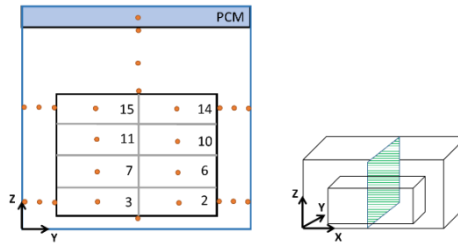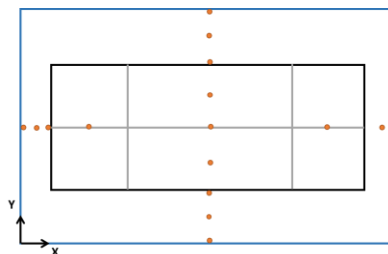

(a)
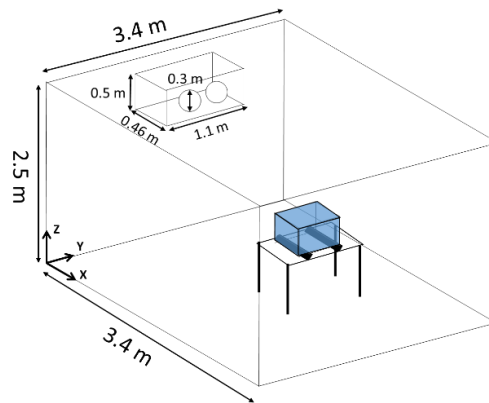
(b)
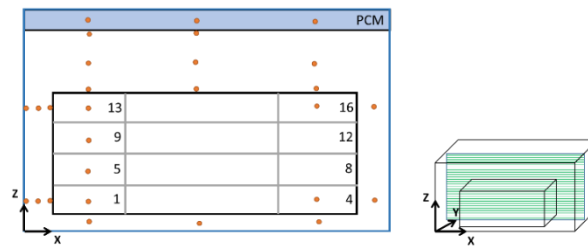
(c)

(d)

(e)

Figure 1: (a) Studied insulated box, (b) experimental set up, (c) test product's arrangement and thermocouple position at front view (XZ plane at Y = 165 mm) (d) test product's arrangement and thermocouple position at side view (YZ plane at X = 255 mm) and (e) test product's arrangement and thermocouple position at top view (the illustrated arrangement was in the case when PCM was at the lid, the similar configuration was applied for the case when PCM was at the side wall with the equal gap between load and PCM and the gap between load and opposite inner wall)

2.1.2.   Instrumentation

Temperature was measured by T-type thermocouples linked to Agilent 34972A data acquisition unit (Agilent Technologies, CA, USA). These thermocouples were previously calibrated at -10°C, 0°C, 10°C, 20°C, 30°C and 40°C with the precision varying from 0.19°C to 0.35°C. Three thermocouples were inserted at the half-thickness of the PCM slab at 3 positions (Fig. 1c). 46 thermocouples were placed inside the box (Fig. 1c to 1e) allowing the measurement of wall, air, product surface and core temperatures. The test products were labelled in number as in Fig. 1c and 1d for interpretation.

2.1.3.   Experimental protocol

PCM slab was placed horizontally in a freezer set at -2°C for at least 48 h before each experiment. In spite of precaution to place PCM slab horizontally in the freezer, PCM thickness varied between 35 mm and 40 mm after completely frozen. Sixteen packs of test product were placed in a polystyrene box before keeping in a domestic refrigerator set at 4°C for at least 24 h prior to each experiment allowing homogenous temperature of the packs despite the "on" and "off" compressor working cycle. The test products and the PCM were placed inside the box rapidly (less than 10 min of manipulation) before closing by the lid, in such a way, the temperatures perturbation was limited during the manipulation.

2.1.4.   Experimental conditions

Four experiments were carried out to study the effect of PCM position and the spacing beneath the load as summarized in Table 1.

Table 1: Experimental conditions

Exp No.	PCM position	Space beneath the load (cm)
1	Lid	0
2	Side wall	0
3	Lid	2
4	Side wall	2

2.2.   Results and discussions

2.2.1.   Temperature evolution in experiment 1 (PCM at lid, without space beneath the load)

Fig. 2 presents the evolution of some temperatures in the insulated box equipped with PCM in experiment 1: PCM half-thickness, PCM surface, internal wall and air around the test product no.13, surface and core temperatures of this product. This evolution can be divided into 3 periods according to the state of PCM: period I (0 min to 100 min) where frozen PCM temperature increased from -2°C to its melting temperature of 0°C and wall temperature decreased from 20°C to around 9°C, period II (100 min to 840 min) where PCM was melting, and its temperature was constant and period III (after 840 min) where PCM was completely melted, and its temperature increased continuously.

During the period I, PCM temperature increased whereas air temperature decreased due to the heat exchange between them. During setup manipulation (ambient temperature around 20°C), the product surface temperature increased up to around 10°C. Once the box was closed (t = 0), the product surface temperatures and the inner wall temperature decreased because the adjacent air became colder.

During the period II, PCM was melting. PCM temperature remained constant in the range between -0.2°C and -0.1°C corresponding to the range of melting point of tap water (Cengel & Ghajar, 2014). During this period, especially before 600 min, all the temperatures remained almost constant, except the product core temperature.

The temperature at internal wall of the box was the highest as there was heat flux from outside. Internal air temperature was about 3°C lower than that at internal wall and about 2°C higher than that at the product surface. This small difference leads to suppose that air flows by natural convection with very low velocity. Comparing internal air temperature beside test product (TC2) and above test product (TC6), air above test product had lower temperature because of the heat exchange with PCM surface. Surface product temperature was also lower above the product compared to side location, this can be explained by the convection with surrounding air and by radiation, respectively with cold PCM surface and warmer lateral inner wall.

The product core temperature was initially near 4°C (it did not vary during setup manipulation) and increased continuously up to around 5°C during periods I and II. This is because it was initially lower than the equilibrium one. The equilibrium temperature is the one which would reach (at a given position) after a long time with the assumption that PCM remains everywhere at its melting temperature (-0.1°C in this experiment). Between 400 and 600 min, the product core temperature variation was low (<0.3°C), and all the air and surface temperature were stable. Therefore, we could estimate steady state was almost reached. After 600 min, the air temperature slightly increased, thus it suggested that some part of the PCM was higher than 0°C and turned into water.

According to the data analysis, temperatures between 400 min and 600 min were considered suitable for further interpretation under "quasi" steady state as the standard deviation of temperature measured during this period was below ±0.3°C (ATP, 2020). Our results are in agreement with the ones of Ge et al. (2014) for

an insulated box which reported different temperature profiles (wall, air, product surface and core) and mentioned that the core temperature of test product was the lowest.

During period III, PCM was completely melted. Its temperature sharply increased because the liquid PCM was heated from the external ambience (Cengel & Ghajar, 2014). Consequently, all temperatures (wall, air and product) increase more significantly than that during period II.
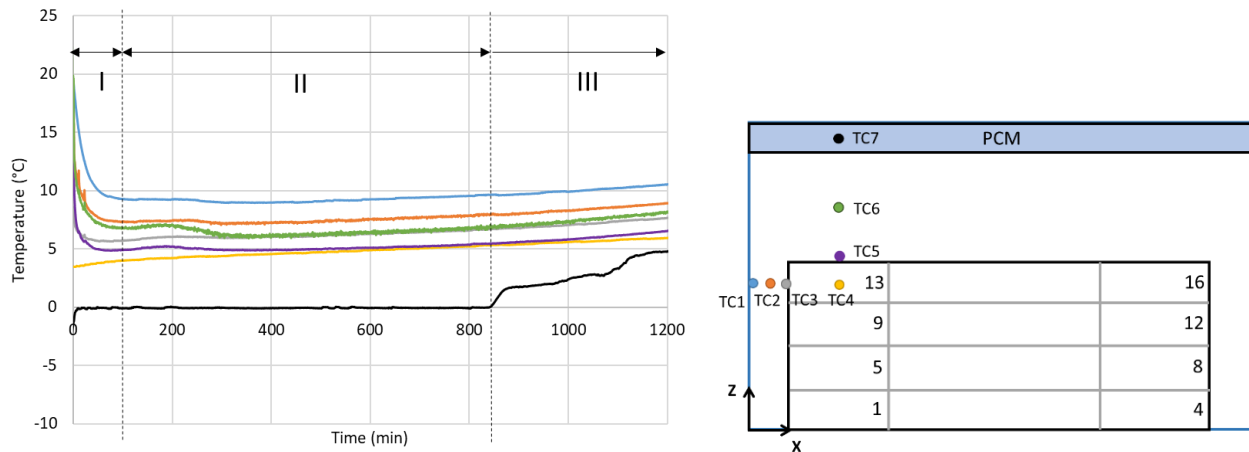

Figure 2: Temperature evolution of Exp No.1 around test product no.13

2.2.2.   Effect of PCM position

Fig 3a to Fig 3d show the temperatures of PCM, internal air and core of test product at different positions during quasi steady state (average value calculated between 400 min and 600 min). Table 3 summarizes the core product temperatures at quasi steady state: mean value, standard deviation, maximum and minimum values for the 14 test product blocks.

When PCM was at the lid of the box (Fig 3a and 3b), the lowest air temperature of 4.4°C was located at the top (between PCM and product) and the warmest air of 7.6°C was located between the product top layer and the side wall. It leads to suppose that after exchanging the heat at PCM surface, the coldest air (high density) flew downward to the bottom. After being heated by warm box wall, air temperature increased (low density) and flew upward to reach PCM surface again. The same airflow pattern was observed in a static domestic refrigerator without fan by Laguerre et al. 2008. There is a difference in air temperature between left and the right sides. This could be explained by a slight difference in wall thickness (perhaps less insulation at right side), or a small dissymmetry in load and/or thermocouples placement. These observations are in agreement with the ones predicted by Rincón-Casado et al. (2017). These authors studied a 2-dimensional rectangular empty cavity with cold plate at the top and warm plate at the bottom (adiabatic side walls). They reported that the coldest area was in the center area below the cold plate while the warmest area was around the side wall.

The product at the center of top layer had the lowest temperature and the one at the corner of bottom layer was the warmest. Even near the warmest air of 7.6°C, the product temperature was relatively low: 5.3 °C notably because of the conduction with the other the product blocs (East & Smale, 2008). The dissymmetry of air temperature also led to a slight dissymmetry in product temperature. The positions of the coolest and warmest product temperature are in agreement with the ones reported by Margeirsson et al. (2011) and Margeirsson et al. (2012). These authors placed ice at the top of a box filled with fish and indicated that the coldest area was at the center of the top level while the warmest area was at the corner of the bottom level.

When PCM was at a side wall of the box (Fig 3c and 3d), the coldest air of 1.2°C was at the bottom of the box close to PCM surface and the warmest air of 8.9°C was at the top of the box. It can be explained by the fact that when the air exchanged heat with PCM surface, its temperature decreased while its density increased, thus, it flew downward, then it flew around the load toward the other lateral walls which were not covered

by PCM, and it gained heat from these box's wall and flew upward until reaching the top. For 2-dimensional rectangular empty cavity with a vertical cold wall opposite to a vertical warm wall (adiabatic top and bottom walls), Rincón-Casado et al. (2017) stated that the coldest area was at the bottom close to the cold plate while the warmest area was around the top close to the warm plate. These observations are in agreement with the ones of our study.

The coldest test product (3.7°C) was close to the coldest air (1.2°C) but at the second layer from the bottom. Indeed, the product at the bottom (4.4°C) received heat from the external ambiance through the bottom box wall (Laguerre et al., 2018). The test product with the highest core temperature of 6.7°C was at the top of the box close to the warm air of 8.5°C.
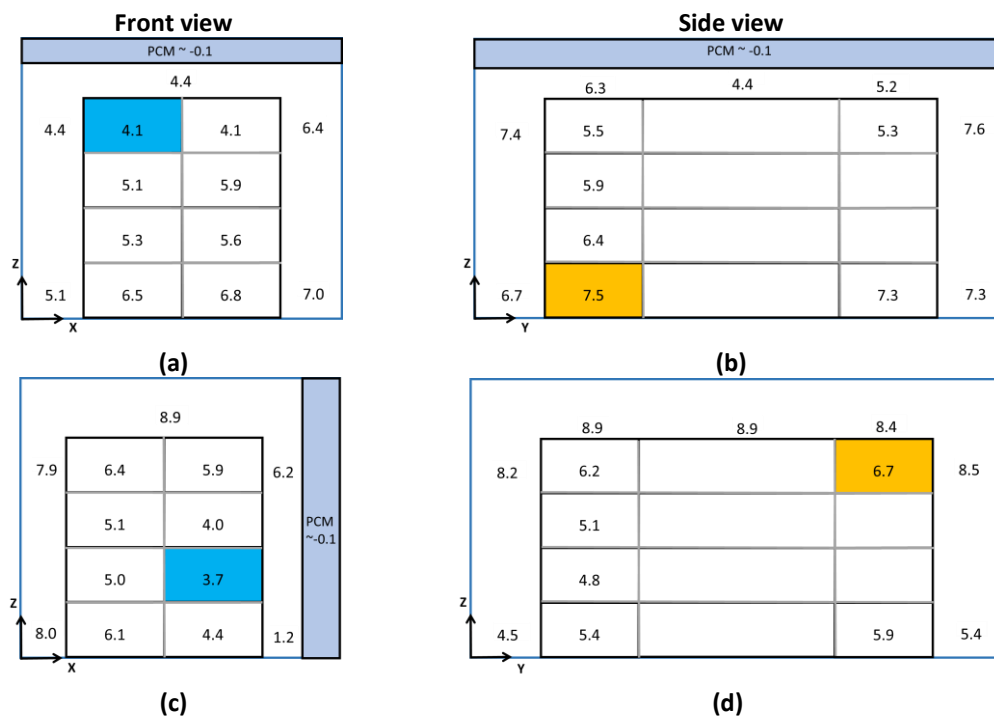

Figure 3: Temperature profile (in °C) at quasi steady state (400 min – 600 min) (a) Exp no.1 – front view, (b) Exp no.1 – side view, (c) Exp no.2 – front view and (d) Exp no.2 – side view (The coldest test product was filled with blue color while the warmest one was filled with orange color)

The effect of PCM position clearly affected the temperature profile and the coldest and warmest position in spite that the average temperature at quasi steady state was almost the same (Table 2). The difference in temperature profile is due to the difference in airflow pattern with PCM at the lid and at the side.

Table 2: Temperature profile at quasi steady state (400 min – 600 min) of each experiment

Exp No.	PCM position / space beneath load	Temperature at quasi steady state in °C (Mean ± SD)	Maximum temperature (°C)	Minimum temperature (°C)
1	Lid / no space	5.7 ± 1.1	7.5	4.1
2	Side wall / no space	5.3 ± 0.9	6.7	3.7
3	Lid / 2 cm space	5.6 ± 0.6	6.5	4.5
4	Side wall / 2 cm space	5.4 ± 0.9	6.8	4.1

2.2.3.   Effect of air space underneath the load

From Table 3, the presence of air space underneath the load had neither influence on average temperature of test products nor the coldest and the warmest position (results not shown). However, the product temperature is more homogeneous in the case of air space (lower difference between maximum and

minimum core temperature). This is because of better convective heat transfer as the air can flow from one side wall to the opposite side.

2.2.4. Optimal condition for transportation in an insulated box

From previous sections, it can be seen that the PCM position affected the temperature profile and the space below the load impacted the difference between the lowest and the highest core temperature. However, none of these factors changed the average temperature at quasi steady state.

During food transportation and storage, average temperature of products is main consideration since it influences the quality and shelf-life of the products (Mercier et al., 2017). Another essential criterion is the temperature homogeneity because it is necessary to ensure that products in different position have the same quality (Laguerre et al., 2013). As a result, the space underneath the load is important to insure homogeneous temperature. In addition, it can be interesting to know the location of the coldest and warmest area if the load is constituted by sensitive products.

3. CONCLUSIONS

This experiment investigated the effect of PCM position and spacing below the load on temperature profile in an insulated box equipped with PCM. While PCM was melting, its temperature, internal air temperature and test product's surface temperature remained constant, but core temperature slowly increased in this period.

PCM position did not clearly impact average product temperature, but it influenced the coldest and warmest position inside the box. Adding the spacing beneath the load decreased the different between the highest and the lowest core temperature. To optimize the transportation and storage in an insulated box equipped with PCM, adding the gap below the load is important to achieve consistent product's quality throughout the box. Gap thickness should be optimized in term of product quality gain and reduction of useful volume. This optimization can be reached by numerical model.

Further experimental and modelling works on air velocity field would be complementary allowing better understanding of the heat transfer phenomena.

ACKNOWLEDGEMENTS

REFERENCES

Bergman, T. L., Lavine, A. S., Incropera, F. P., & DeWitt, D. P. (2011). Introduction to Heat Transfer. John Wiley & Sons.

Cengel, Y., & Ghajar, A. (2014). Heat and Mass Transfer: Fundamentals and Applications (5th edition). McGraw-Hill Education.

Chaomuang, N., Laguerre, O., & Flick, D. (2020). A simplified heat transfer model of a closed refrigerated display cabinet. Thermal Science and Engineering Progress, 17, 100494. https://doi.org/10.1016/j.tsep.2020.100494

Du, J., Nie, B., Zhang, Y., Du, Z., Wang, L., & Ding, Y. (2020). Cooling performance of a thermal energy storage-based portable box for cold chain applications. Journal of Energy Storage, 28, 101238. https://doi.org/10.1016/j.est.2020.101238

East, A., & Smale, N. (2008). Combining a hybrid genetic algorithm and a heat transfer model to optimise an insulated box for use in the transport of perishables. Vaccine, 26(10), 1322–1334. https://doi.org/10.1016/j.vaccine.2007.12.055

Ge, C., Cheng, Y., & Li, B. (2014). Numerical simulation and experimental study of the heat transition in a foam container. Journal of Cellular Plastics, 50(1), 15–36. https://doi.org/10.1177/0021955X13503846

Harvey, P. D., & American Society for Metals (Eds.). (1982). Engineering properties of steel. American Society for Metals.

Hundy, G. F., Trott, A. R., & Welch, T. C. (2008). Chapter 15—Cold Storage. In G. F. Hundy, A. R. Trott, & T. C. Welch (Eds.), Refrigeration and Air-Conditioning (Fourth Edition) (pp. 184–197). Butterworth-Heinemann. https://doi.org/10.1016/B978-0-7506-8519-1.00015-3

Laguerre, O., Ben Amara, S., Charrier-Mojtabi, M.-C., Lartigue, B., & Flick, D. (2008). Experimental study of air flow by natural convection in a closed cavity: Application in a domestic refrigerator. Journal of Food Engineering, 85(4), 547–560. https://doi.org/10.1016/j.jfoodeng.2007.08.023

Laguerre, O., Derens, E., & Flick, D. (2018). Modelling of fish refrigeration using flake ice. International Journal of Refrigeration, 85, 97–108. https://doi.org/10.1016/j.ijrefrig.2017.09.014

Laguerre, O., Hoang, H. M., & Flick, D. (2013). Experimental investigation and modelling in the food cold chain: Thermal and quality evolution. Trends in Food Science & Technology, 29(2), 87–97. https://doi.org/10.1016/j.tifs.2012.08.001

Margeirsson, B., Gospavic, R., Pálsson, H., Arason, S., & Popov, V. (2011). Experimental and numerical modelling comparison of thermal performance of expanded polystyrene and corrugated plastic packaging for fresh fish. International Journal of Refrigeration, 34(2), 573–585. https://doi.org/10.1016/j.ijrefrig.2010.09.017

Margeirsson, B., Pálsson, H., Popov, V., Gospavic, R., Arason, S., Sveinsdóttir, K., & Jónsson, M. þór. (2012). Numerical modelling of temperature fluctuations in superchilled fish loins packaged in expanded polystyrene and stored at dynamic temperature conditions. International Journal of Refrigeration, 35(5), 1318–1326. https://doi.org/10.1016/j.ijrefrig.2012.03.016

Mercier, S., Villeneuve, S., Mondor, M., & Uysal, I. (2017). Time-Temperature Management Along the Food Cold Chain: A Review of Recent Developments: Food preservation along the cold chain…. Comprehensive Reviews in Food Science and Food Safety, 16. https://doi.org/10.1111/1541-4337.12269

Navaranjan, N., Fletcher, G. C., Summers, G., Parr, R., & Anderson, R. (2013). Thermal insulation requirements and new cardboard packaging for chilled seafood exports. Journal of Food Engineering, 119(3), 395–403. https://doi.org/10.1016/j.jfoodeng.2013.05.042

Rincón-Casado, A., Sánchez de la Flor, F. J., Chacón Vera, E., & Sánchez Ramos, J. (2017). New natural convection heat transfer correlations in enclosures for building performance simulation. Engineering Applications of Computational Fluid Mechanics, 11(1), 340–356. https://doi.org/10.1080/19942060.2017.1300107

ATP. (2020). Agreement on the International Carriage of Perishable Foodstuffs and on the Special Equipment to be Used for Such Carriage: (ATP) as amended 6 July 2020. United Nations. https://doi.org/10.18356/6fa10b27-en

Zhao, X., Xia, M., Wei, X., Xu, C., Luo, Z., & Mao, L. (2019). Consolidated cold and modified atmosphere package system for fresh strawberry supply chains. LWT, 109, 207–215. https://doi.org/10.1016/j.lwt.2019.04.032